Valley selection rule in a Y-shaped zigzag graphene nanoribbon junction*

Zhang Lin(张 林)[a)†] and Wang Jun(汪 军)[b)]

[a)] *Department of Applied Physics, College of Science, Nanjing Forestry University, Nanjing* 210037, *China*
[b)] *Department of Physics, Southeast University, Nanjing* 210096, *China*

(Received 15 November 2013; revised manuscript received 14 February 2014; published online 10 June 2014)

The valley valve effect was predicted in a straight zigzag graphene nanoribbon (ZGR) p/n junction. In this work, we address a possible valley selection rule in a Y-shaped ZGR junction. By modeling the system as a three-terminal device and calculating the conductance spectrum, we found that the valley valve effect could be preserved in the system and the Y-shaped connection does not mix the valley index or the pseudoparities of quasiparticles. It is also shown that the Y-shaped ZGR device can be used to separate spins in real space according to the unchanged valley valve effect. Our finding might pave a way to manipulate and detect spins in a multi-terminal graphene-based spin device.

Keywords: valley selection rule, zigzag graphene nanoribbon, pseudoparity, conductance

PACS: 72.25.Dc, 72.80.Vp, 72.25.Mk **DOI:** 10.1088/1674-1056/23/8/087202

1. Introduction

Graphene, an attractive material for spintronics, has received much attention due to its unique band structure and novel electron transport properties,[1–12] such as long spin relaxation length,[5,6] high carrier mobility,[1,7] and gate tunable spin transport.[8–10] Among these properties, the spin filtering effect is especially intriguing, which indicates the possibility of high controllability of spin manipulation in graphene. Since Dmitry *et al.*[13] firstly predicted the spin filtering effect in the magnetic graphene, many researchers utilized magnetic graphene junctions to design various types of graphene spin valves or spin filter devices.[14–17] For instance, Zhang *et al.*[14] theoretically studied the giant magnetoresistence effect in a ferromagnetic (F) graphene junction, and found that the nanoribbon can act as a perfect spin filter. Subsequently, Michetti and his coworker[15] investigated a bilayer graphene contacted to F insulators, which can be devised as highly efficient gate-tunable spin filters. In recent works,[18,19] a zigzag graphene nanoribbon (ZGR) junction together with ferromagnetism was found not only as a spin injector to generate spin polarized carriers, but as a spin splitter to separate spins in real space. Spin detection in magnetic graphene junctions has also been studied theoretically[20,21] and experimentally.[22,23] For example, Wang *et al.*[21] theoretically proposed an even-chain ZGR junction with a rotating magnetic field to separate and detect a fully spin-polarized current spatially. McCreary *et al.*[22] reported experimentally a pure spin current measured by its induced magnetic moments in a graphene-based spin valve.

As an analogy to the spin valve effect in a magnetic tunneling junction, the peculiar valley-valve effect[24–26] was revealed in a nonmagnetic p/n ZGR junction. The intrinsic inter-valley electron scattering process crucially relies on the zigzag-chain number N for the case of the zero-energy transport mode: when N is even, electrons are completely reflected and the current is blocked; oppositely, the current is allowed in an antizigzag junction when N is odd. This peculiar current blocking phenomenon is attributed to the pseudoparity conservation called the valley selection rule. The wavefunctions of the quasiparticles have a definite valley index or pseudoparity, and they would be different for the p-doped and n-doped ZGR. Therefore, only the quasiparticles with the same pseudoparities are allowed to pass through the p/n junction; whereas the quasiparticles are blocked to transport with the opposite pseudoparities in each region. This additional valley degree of freedom provides the possibility of manipulating and controlling the electron transport in graphene-based devices.

The previous works[27–30] on the valley-valve effect were mainly focused on a straight even-chain ZGR junction, and the valley degree of freedom is related to the electron momentum, so whether the valley-valve effect exists in a nonstraight even-chain ZGR junction or not is worthy of study. Thus in this work, we propose an even-chain Y-shaped ZGR p/n junction in Fig. 1 to study the valley-valve effect. By using the multi-terminal Landauer–Bütticker formula, we calculated the conductance spectrum of the system and found that the valley-valve effect could still be preserved, because the connection of the Y-shape composed of a hexagonal honeycomb lattice does not bring out the valley-mixing scattering and the pseudoparities of particles remain unchanged. As an example, the ferro-

*Project supported by the National Natural Science Foundation of China (Grant No. 110704033), the Natural Science Foundation of Jiangsu Province, China (Grant No. BK2010416), and the Natural Science Foundation for Colleges and Universities in Jiangsu Province, China (Grant No. 13KJB140005).

†Corresponding author. E-mail: lzhang2011@gmail.com

© 2014 Chinese Physical Society and IOP Publishing Ltd

magnetic (F) version of the Y-shaped ZGR junction is studied to separate spins spatially by using the unchanged valley-valve effect.

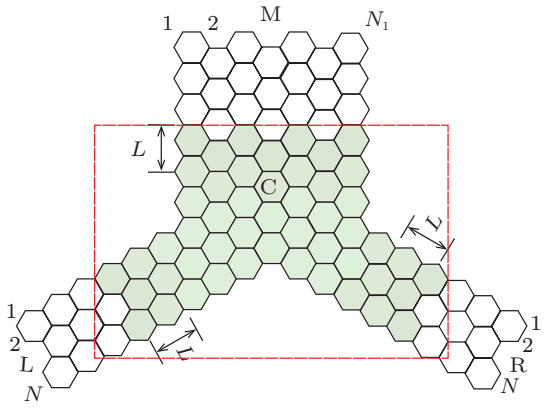


Fig. 1. (color online) Schematic plot of a Y-shaped ZGR p/n junction. The nonstraight C region (in red-dashed box) is an undoped ZGR, while the left (L), the middle (M), and the right (R) ZGRs are three semi-infinite p-doped or n-doped ZGR leads. The widths of the left (right) and middle ZGRs are respectively N and N_1, while the length of the C region is described by L.

The rest of this paper is arranged as follows. In Section 2, we present the theoretical model for the proposed even-chain Y-shaped ZGR junction and derive a general formulae for the conductance spectrum of the device. In Section 3, numerical results are presented to illustrate the valley-valve effect in the nonstraight Y-shaped ZGR p/n junction. Finally, a brief conclusion is drawn in Section 4.

2. Model and formulation

We consider a three-terminal Y-shaped ZGR p/n junction as illustrated in Fig. 1, where the C region is an undoped ZGR connecting to the three ZGR leads. The left (L), the middle (M), and the right (R) ZGRs are three p-doped or n-doped leads with controllable potentials $U_{\mathrm{L(M,R)}}$. The widths of the left (right) and middle ribbons are denoted by the zigzag-chain numbers N and N_1, respectively; the length of the C region is La with the lattice constant $a = 2.46$ Å. In the tight-binding model, the system's Hamiltonian is given by

$$H = \sum_{i\alpha\sigma\sigma'} C^{\dagger}_{i\alpha\sigma}(U_{\alpha}\delta_{\sigma\sigma'})C_{i\alpha\sigma'} - t\sum_{\langle ij\rangle\alpha\sigma} C^{\dagger}_{i\alpha\sigma}C_{j\alpha\sigma} + \mathrm{c.c.} + \sum_{i\sigma} C^{\dagger}_{i\sigma}(w_{ic})C_{i\sigma}, \quad (1)$$

where $C^{\dagger}_{i\alpha\sigma}$ ($C_{i\alpha\sigma}$) is the creation (annihilation) operator at the lattice site i with spin index σ ($\sigma = \pm = \uparrow\downarrow$) of the α ($\alpha =$ L, M, R, C) ZGR in real space; U_{α} is the on-site energy of the α ZGR in the Y-shaped ZGR p/n junction, which can be modulated by gate voltages. The $\langle ij\rangle$ means the nearest neighbor lattice sites i and j. $t = 2.8$ eV is the hopping integral.[31] The last term describes the disordering lattice potential in the C region, w_{ic} represents the random disorder uniformly distributed in the range $[-W/2, W/2]$, where W is the disorder strength. The linear conductance in our proposed device can be obtained by using the multi-terminal Landauer–Bütikker formula,[32,33] which reads

$$G_{\alpha\beta}(E) = \frac{2e^2}{h}\mathrm{Tr}[\Gamma_{\alpha}G^{\mathrm{r}}(E)\Gamma_{\beta}G^{\mathrm{a}}(E)], \quad (2)$$

where the trace Tr denotes the summation over all the transverse lattice site i on the surface of the C region. $G^{\mathrm{r}} = [G^{\mathrm{a}}]^{\dagger}$ is the retarded (advanced) Green function in real space, which can be calculated by the direct matrix inversion

$$G^{\mathrm{r}} = [EI - H_{\mathrm{C}} - \Sigma^{\mathrm{r}}_{\mathrm{L}} - \Sigma^{\mathrm{r}}_{\mathrm{R}} - \Sigma^{\mathrm{r}}_{\mathrm{M}}]^{-1}, \quad (3)$$

where H_{C} is the Hamiltonian of the nonstraight C region in real space, and I is a unitary matrix. The contributions of the three semi-infinite ZGR leads are incorporated by the three self-energy terms $\Sigma^{\mathrm{r}}_{\alpha}$, which can be evaluated by the recursive Green function method.[34,35]

With these preparations, the conductance spectrum of the system can be worked out directly

$$G_{\mathrm{ML(R)}}(E) = \frac{2e^2}{h}\mathrm{Tr}[\Gamma_{\mathrm{M}}G^{\mathrm{r}}_{\mathrm{ML(R)}}(E)\Gamma_{\mathrm{L(R)}}G^{\mathrm{a}}_{\mathrm{L(R)M}}(E)], \quad (4)$$

$$G_{\mathrm{LR}}(E) = \frac{2e^2}{h}\mathrm{Tr}[\Gamma_{\mathrm{L}}G^{\mathrm{r}}_{\mathrm{LR}}(E)\Gamma_{\mathrm{R}}G^{\mathrm{a}}_{\mathrm{RL}}(E)]. \quad (5)$$

Here $\Gamma_{\alpha} = \mathrm{i}[\Sigma^{\mathrm{r}}_{\alpha} - \Sigma^{\mathrm{a}}_{\alpha}]$ is the linewidth function, which indicates the transmission strength between the α terminal and the non-straight C region. $G_{\alpha\beta}(E)$ is the conductance between the α and β terminals, which is mainly dependent on the Fermi energy E_{F} in Eqs. (4) and (5). If the nonstraight ZGR connection has no effect on the pseudoparities conservation of the quasiparticles, the peculiar valley-valve effect should emerge in the studied Y-shaped ZGR p/n junction, and the conductances can be allowed (closed) for the quasiparticles with the same (opposite) pseudoparities due to the persistent valley selection rule.

3. Numerical results and discussion

In this section, we shall present the numerical results of the conductances in an even-chain Y-shaped ZGR junction and analyze the behavior of the valley selection rule. Since three terminals of the device are asymmetric, the width of the middle ZGR lead is 2 times the left or right ZGR lead, we mainly focus on the conductance of the middle-left (right) terminal. In numerical calculations, the zero temperature ($T = 0$ K) is taken, the even-chain ZGR is considered and the widths of the middle and left (right) ZGR leads are set as N_1 and N, and which satisfies $N_1 = 2N$. The three ZGR terminals have the same potentials assumed $|U_{\mathrm{L}}| = |U_{\mathrm{M}}| = |U_{\mathrm{R}}| = U = 0.05$ eV, and $U_{\mathrm{C}} = 0$ eV is set as the zero energy reference. In most cases unless otherwise stated directly, the ZGR junction is perfect $w_{ic} = 0$ eV, and the length and the width of the non-straight C region are $L = 50$ and $N = 4$, respectively.

In Fig. 2, we calculate the conductance $G_{\mathrm{ML(R)}}$ versus E_{F} to reveal whether the valley-valve effect could appear in a nonstraight ZGR p/n junction or not. When the right ZGR lead is n-doped and the left ZGR lead has the same p-doped as the middle ZGR lead in Fig. 2(a), similar to the straight ZGR p/n junction case, the valley valve effect emerges at $-U < E_{\mathrm{F}} < 0$, the particles can only pass through the middle-left electrode. G_{ML} is nonzero and oscillating with the Fermi energy; whereas the middle-right terminal is closed for the particles transport, i.e., $G_{\mathrm{MR}} = 0$. The opposite phenomenon happens in Fig. 2(b) when the right ZGR has the same p-doped and the left ZGR is n-doped type, the conductances, the ON or OFF states, are reversed between the middle-left and middle-right terminals in comparison with results in Fig. 2(a), $-U < E_{\mathrm{F}} < 0$, $G_{\mathrm{ML}} = 0$, and $G_{\mathrm{MR}} = 1$. Therefore, the valley valve effect is preserved in a nonstraight Y-shaped ZGR p/n junction. This indicates that the Y-shaped ZGR connection does not lead to the valley-mixing scattering and makes no difference to the pseudoparities conservation of particles.

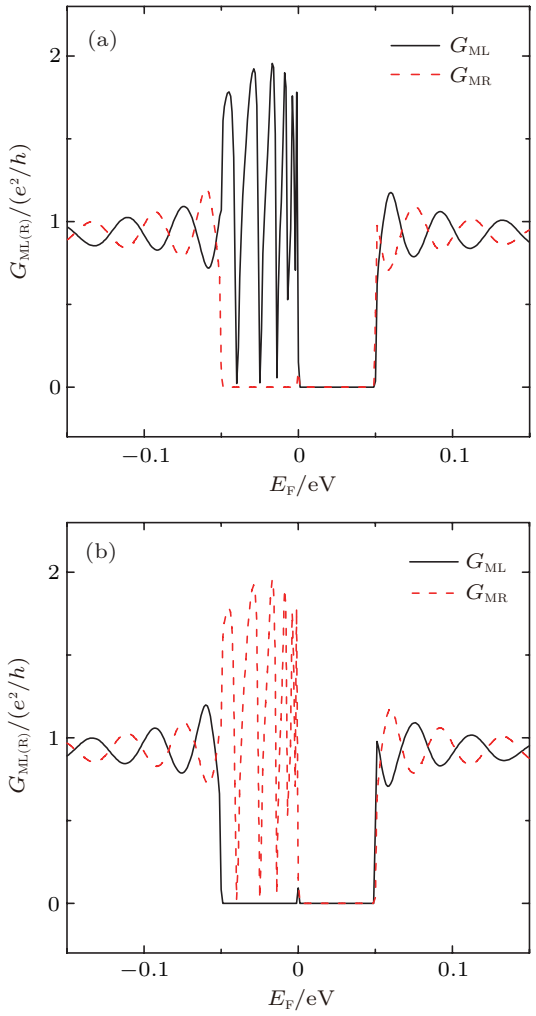


Fig. 2. (color online) Conductance $G_{\mathrm{ML(R)}}$ versus Fermi level E_{F} in a Y-shaped ZGR p/n junction, the on-site energies of the left, the middle, and the right ZGR leads are $U_{\mathrm{R}} = -0.05$, $U_{\mathrm{L}} = U_{\mathrm{M}} = 0.05$ eV in panel (a) and $U_{\mathrm{L}} = -0.05$, $U_{\mathrm{R}} = U_{\mathrm{M}} = 0.05$ eV in panel (b).

To explain the persistent valley-valve effect in the Y-shaped ZGR p/n junction in Figs. 2(a) and 2(b), we plot the zero-energy transport modes of the middle, the C, and the left (right) ZGRs in the momentum k-space in Figs. 3(a) and 3(b). The p (n)-doped energy bands of the middle and the left (right) terminals move upward (downward) from the undoped C region, which may cause the electrons and holes in the middle, the C, the left (right) ZGR regions possessing the opposite even ("+") and odd ("−") pseudoparities near the Fermi level. These definite "±" pseudoparities of particles at each terminal are not affected by the nonstraight ZGR connection, and the valley selection rule is still valid in a multi-channel ZGR junction. When the left and middle ZGRs have the same p-doped type in Fig. 3(a), the quasiparticles in the middle, the C, and the left ZGRs have the same pseudoparities at $-U < E_{\mathrm{F}} < 0$, the valley transport process is allowed and $G_{\mathrm{ML}} \neq 0$ in Figs. 2(a). When the left and middle ZGRs have the opposite type in Figs. 3(b), the quasiparticles in the left, middle, and C regions have the opposite pseudoparities at $-U < E_{\mathrm{F}} < U$, the middle-left channel is closed for the transmission and $G_{\mathrm{ML}} = 0$ in Fig. 2(b).

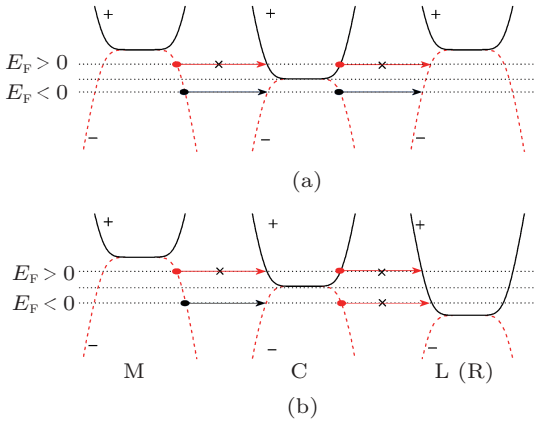


Fig. 3. (color online) E–K dispersion of zero-energy edge states of the middle C and left (right) ZGRs. The left (right) lead is same p-doped (a) or opposite n-doped (b) with the middle lead. The "+" and "−" denote the even and odd pseudoparities of the edge states, and it could be different for the conduction band (solid line) and the valence band (dashed line), respectively. The arrows indicate the quasiparticle transmission due to the valley selection rule.

We also consider the possible effects of the nonstraight C region on the persistent valley selection rule. Figure 4 describes G_{MR} versus E_{F} with different device sizes and disorder potentials W in the Y-shaped ZGR p/n junction. Two different sizes of the device are considered in Fig. 4(a), one type has a different length L with a constant width N, the other has a different N and a fixed L. As predicted, although the transmission conductance is crucially dependent on the device width N, these two types of C region would not affect the valley valve effect at $-U < E_{\mathrm{F}} < U$; the conductance is always in the OFF state ($G_{\mathrm{MR}} = 0$) regardless of the device sizes, while the conductance exhibits a transmission peak in the vicinity of $E_{\mathrm{F}} = 0$, and the transmission strength decreases

with the scattering length L. Figure 4(b) shows that the valley selection rule is influenced by the disorder potential W. When $-U < E_F < U$ and W is weak, the valley selection rule is unchanged and $G_{MR} \approx 0$ compared with the perfect ZGR junction $W = 0$. When the disorder potential increases and has the approximate magnitude of the on-site energy of the ZGR, i.e., $W \sim U$, it will destroy the pseudoparity conservation of quasiparticles and the conductance shows the ON state, $G_{MR} \neq 0$. Therefore, as long as the nonstraight C region is clean or has weak disorder potential, the valley selection rule can appear in the Y-shaped ZGR p/n junction.

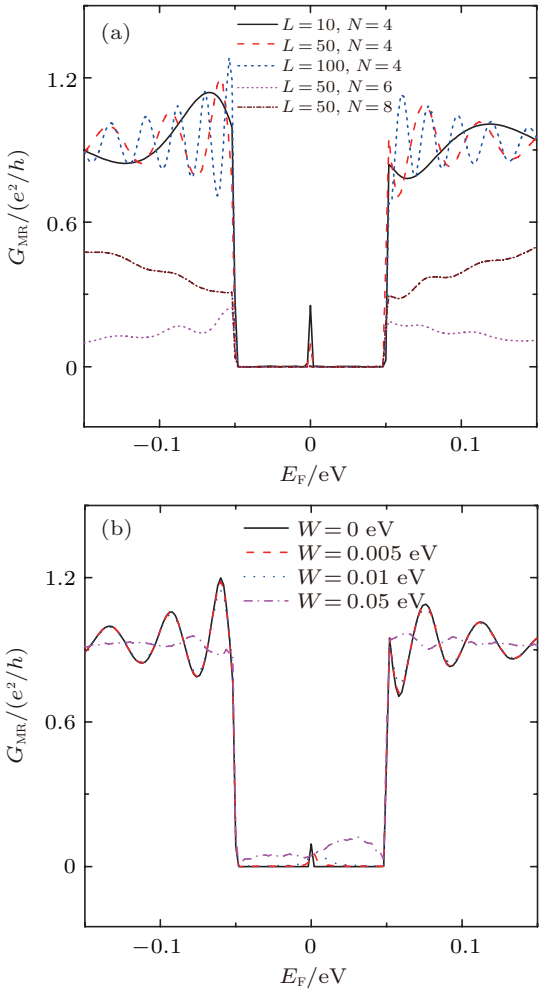


Fig. 4. (color online) Conductance G_{MR} versus Fermi level E_F in a Y-shaped p/n junction, the different lengths and widths of the nonstraight C region $L = 10$, 50, 100, and $N = 4$, 6, 8 are considered in panel (a) and the disorder potential strength $W = 0$, 0.005, 0.01, 0.05 eV in panel (b). The other parameters are the same as those in Fig. 2(a).

As an example of the application of the unchanged valley selection rule in the proposed ZGR junction, we propose the Y-shaped ZGR F/N/F junction to separate and detect spins. It is assumed the equal F magnetization could be induced in the left, the middle, and the right terminals with the magnitude h, while the magnetization angles are denoted by θ_L, θ_M, and θ_R against the z axis, respectively. Thanks to the Zeeman effect, the spin-up and spin-down energy bands are split and they may have the opposite pseudoparities at different terminals. The ferromagnetic ZGR junction becomes a bipolar spin half-metal that only one spin-state channel is open through the middle-left terminal with the same pseudoparities, the opposite spin-state with the opposite pseudoparity is closed while it may be allowed to the middle-right terminal, so the Y-shaped ZGR F/N/F junction would be used as a spin separator and detector.

According to the persistent valley-valve effect in Fig. 5, we present the spin-resolved conductances $G_{ML\sigma}$ and $G_{MR\sigma}$ versus E_F in the Y-shaped F/N/F junction to realize spin separation and detection. When the left and the middle ZGRs have the same magnetization direction $\theta_L = \theta_M = 0$ in Fig. 5(a), the middle-left terminal becomes a spin-half metal at $-h < E_F < h$ that only one spin-species conductance is nonzero, and thus it can be used to detect spin. When $-h < E_F < 0$, due to the pseudoparity conservation, the middle-left terminal is open for the spin-up particles ($G_{ML\uparrow} \neq 0$) and closed for the spin-down ones ($G_{ML\downarrow} = 0$). The opposite spin separation process occurs

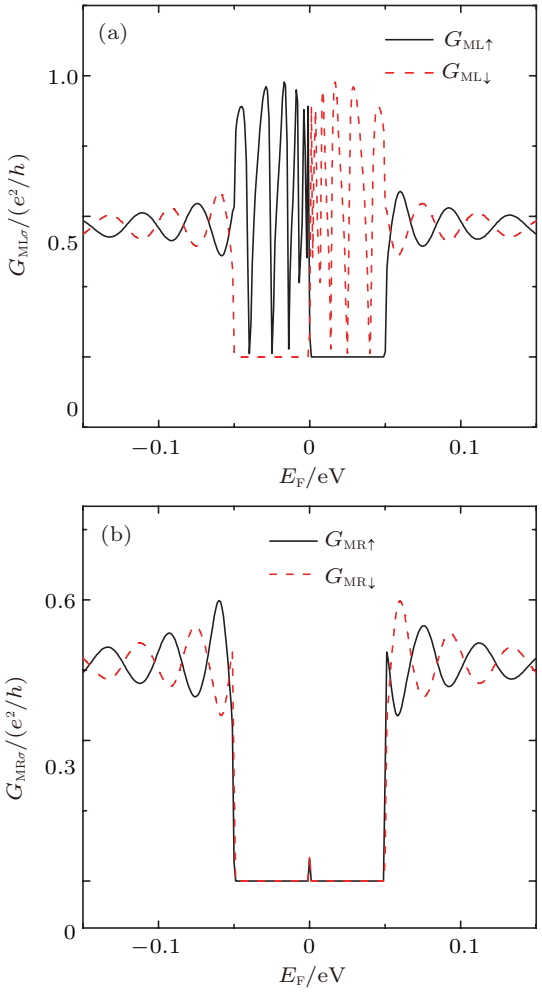


Fig. 5. (color online) (a) Spin-dependent conductances $G_{ML\sigma}$ (a) and $G_{MR\sigma}$ (b) versus E_F in a Y-shaped ZGR F/N/F junction. The left, middle, and right ZGR leads have the same magnetization strength $h = 0.05$ eV, and different magnetization angles: $\theta_L = 0$, $\theta_M = 0$, and $\theta_R = \pi$. The other parameters are: $U_L = U_M = U_R = 0$ eV.

when $0 < E_F < h$, i.e., the spin-up conductance is zero whereas the spin-down tunneling process is allowed, $G_{ML\uparrow} = 0$ and $G_{ML\downarrow} \neq 0$. Similar results occur in the middle-right electrode, as shown in Fig. 5(b), the right ZGR lead has the opposite magnetization orientation $\theta_R = \pi$ to the middle lead, the spin-up and spin-down conductances are both suppressed at $-h < E_F < h$. Therefore, as a spatial spin separator and detector, the Y-shaped ZGR F/N/F junction could spontaneously separate the spin-up and the spin-down electrons into its left and right terminals by matching the unchanged pseudoparity conservation with the middle ZGR terminal, respectively.

Furthermore, the valley–valve effect and spin separation can be effectively controlled by the device parameters in the Y-shaped ZGR F/N/F junction. Figure 6 depicts the spin conductance $G_{MR\sigma}$ versus the magnetization strength h with different magnetization angle θ_R and Fermi level in the junction. It is shown that the unchanged valley-valve effect and its induced spin separation crucially rely on both θ_R and E_F. When $h < |E_F|$, the spin valley-valve effect does not appear, $G_{MR\uparrow}$ and $G_{MR\downarrow}$ are both nonzero and have the same magnitudes approximately; as a result, two spin species cannot be separated. When $h > |E_F|$, only in the parallel configuration $\theta_R = 0$, the Y-shaped ZGR F/N/F junction can act as a bipolar spin separator due to the preserved valley-valve effect. In Fig. 6(a), $G_{MR\uparrow}$ is approximately a constant, and $G_{MR\downarrow}$ is completely suppressed. The middle-right terminal is open for spin-down particles and is closed for spin-up ones when E_F changes its sign in Fig. 6(c). In the antiparallel configuration $\theta_R = \pi$ in Figs. 6(b) and 6(d), both $G_{MR\uparrow}$ and $G_{MR\downarrow}$ are independent of E_F and suppressed at $h > |E_F|$, that is, $G_{MR\uparrow} = G_{MR\downarrow} = 0$, which means the valley-valve effect and its induced spin separation are crucially dependent on the local magnetization distribution and Fermi level in the Y-shaped ZGR F/N/F junction.

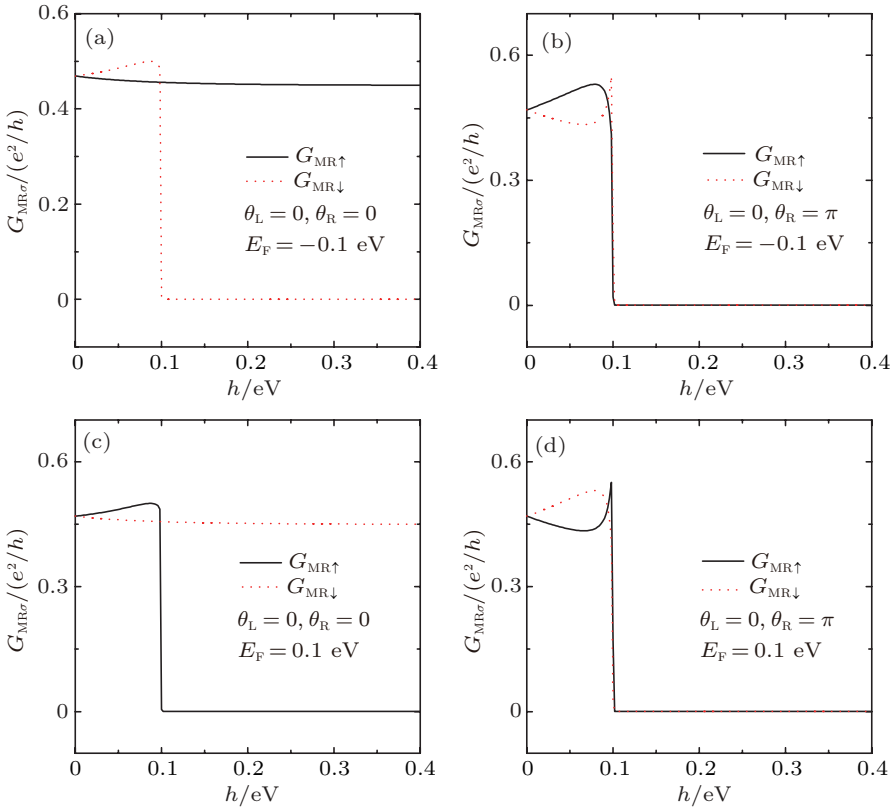


Fig. 6. (color online) Spin conductance $G_{MR\sigma}$ versus magnetization strength h for different Fermi level E_F and different magnetization configurations: (a) $\theta_L = \theta_R = 0$ and $E_F = -0.1$ eV, (b) $\theta_L = 0$, $\theta_R = \pi$ and $E_F = -0.1$ eV, (c) $\theta_L = \theta_R = 0$ and $E_F = 0.1$ eV, and (d) $\theta_L = 0$, $\theta_R = \pi$ and $E_F = 0.1$ eV. The other parameters are set as follows: $\theta_M = 0$ and $U_L = U_M = U_R = 0$ eV.

4. Summary and conclusion

In summary, we have studied the valley selection rule in a nonstraight Y-shaped ZGR p/n junction by calculating the conductance spectrum of the system. It was found that the nonstraight Y-shaped connection has little effect on the pseudoparity conservation of the quasiparticles, so the valley-valve effect is also feasible and depends on the width of each ZGR lead as well as the doping level. The Y-shaped ZGR F/N/F junction was further studied to separate and detect spins by using the unchanged valley-valve effect. Our results may shed light on controlling spins in a multi-terminal graphene-based spin device.

References

[1] Novoselov K S, Geim A K, Morozov S V, Jiang D, Zhang Y, Dubonos S V, Grigorieva I V and Firsov A A 2004 *Science* **306** 666

[2] Novoselov K S, Geim A K, Morozov S V, Jiang D, Katsnelson M I, Grigorieva I V, Dubonos S V and Firsov A A 2005 *Nature* **438** 197

[3] Castro Neto A H, Guinea F, Peres N M R, Novoselov K S and Geim A K 2009 *Rev. Mod. Phys.* **81** 109

[4] Munoz-Rojas F, Fernandez-Rossier J and Palacios J J 2009 *Phys. Rev. Lett.* **102** 136810

[5] Tombros N, Jozsa C, Popinciuc M, Jonkman H T and van Wees B J 2007 *Nature* **448** 571

[6] Wang L and Wu M W 2013 *Phys. Rev. B* **87** 205416

[7] Shishir R S and Ferry D K 2009 *J. Phys.: Condens. Matter* **21** 232204

[8] Han W, Pi K, McCreary K M, Li Y, Wong J J I, Swartz A G and Kawakami P K 2010 *Phys. Rev. Lett.* **105** 167202

[9] Kechedzhi K, Hwang E H and Das Sarma S 2012 *Phys. Rev. B* **86** 165442

[10] Zhang Z H, Chen C F and Guo W L 2009 *Phys. Rev. Lett.* **103** 187204

[11] Guo Y F, Guo W L and Chen C F 2010 *J. Phys. Chem. C* **114** 13098

[12] Guo Y F and Guo W L 2012 *J. Appl. Phys.* **111** 074317

[13] Dmitry A A, Lee Patrick A and Levitov S 2006 *Phys. Rev. Lett.* **96** 176803

[14] Zhang Y T, Jiang H, Sun Q F and Xie X C 2010 *Phys. Rev. B* **81** 165404

[15] Michetti P and Recher P 2011 *Phys. Rev. B* **84** 125438

[16] Dell'Anna L and De Martino A 2009 *Phys. Rev. B* **80** 155416

[17] Ding K H, Zhu Z G and Berakdar J 2011 *Phys. Rev. B* **84** 115433

[18] Wang Z F, Jin S and Liu F 2013 *Phys. Rev. Lett.* **111** 096803

[19] Zhang L 2013 *J. Phys.: Condens. Matter* **25** 035303

[20] Valenzuela Sergio O 2009 *Int. J. Mod. Phys. B* **23** 2413

[21] Wang J, Tian H Y, Yang Y H and Chan K S 2012 *Phys. Rev. B* **86** 081404

[22] McCreary K M, Swartz A G, Han W, Fabian J and Kawakami R K 2012 *Phys. Rev. Lett.* **109** 186604

[23] Vera-Marun I J, Ranjan V and van Wees B J 2012 *Nat. Phys.* **8** 313

[24] Rycerz A, Tworzydlo J and Beenakker C W J 2007 *Nat. Phys.* **3** 172

[25] Akhmerov A R, Bardarson J H, Rycerz A and Beenakker C W J 2008 *Phys. Rev. B* **77** 205416

[26] Cresti A, Grosso G and Parravicini G P 2008 *Phys. Rev. B* **77** 233402

[27] Nakabayashi J, Yamamoto D and Kurihara S 2009 *Phys. Rev. Lett.* **102** 066803

[28] Xing Y X, Wang J and Sun Q F 2011 *Phys. Rev. B* **83** 205418

[29] Tian H Y and Wang J 2012 *Chin. Phys. B* **21** 017203

[30] Wang J, Zhang L and Chan K S 2011 *Phys. Rev. B* **83** 125425

[31] Pisani L, Chan J A, Montanari B and Harrison N M 2007 *Phys. Rev. B* **75** 064418

[32] Datta S 1995 *Electronic Transport in Mesoscopic Systems*, 2nd edn. (Cambridge: Cambridge University Press) p. 102

[33] Maher M Kh, Shahtahmassebi N and Roknabadi M R 2013 *Physica E* **54** 93

[34] Li T C and Lu S P 2008 *Phys. Rev. B* **77** 085408

[35] Libisch F, Rotter S and Burgdörfer J 2012 *New J. Phys.* **14** 123006